Journal of Applied Mathematics & Bioinformatics, vol.6, no.3, 2016, 1-21
ISSN: 1792-6602 (print), 1792-6939 (online)
Scienpress Ltd, 2016

Target Detection in Sonar Images using morphological operations and Empirical Mode Decomposition

Apostolos P. Leros[1] and Antonios S. Andreatos[2]

Abstract

Empirical Mode Decomposition (EMD) is a signal decomposition technique particularly suitable for non-stationary and non-linear signals. In this paper, two target detection methods with improved accuracy in side scan sonar images are proposed. In the first method, target detection is based on morphological operations; the second method combines Empirical Mode Decomposition (EMD) with morphological operations. Both methods are enhanced with edge detection filtering. Experimental results indicate that the proposed methods are very effective, but their efficiency depends on the input image. Hence, they should be used in combination.

[1] Department of Automation, School of Technological Applications, Technological Educational Institute of Sterea Hellas, 34400 Psachna, Evia, Greece.
E-mail: lerosapostolos@gmail.com
[2] Div. of Computer Engineering \& Information Science, Hellenic Air Force Academy, Dekeleia Air Force Base, Dekeleia, Attica, TGA-1010, Greece.
E-mails: informatics.hafa@haf.gr, aandreatos@gmail.com

Article Info: *Received* : October 12, 2015. *Revised* : December 18, 2015.
Published online : December 20, 2016.

Mathematics Subject Classification: 94A08

Keywords: Target Detection; side-scan sonar images; morphological operations; Empirical Mode Decomposition; Intrinsic Mode Functions; edge detection; Matlab

1 Introduction

1.1 Sonar mapping systems

Acoustics is the best and often the only means to investigate the water column and seabed efficiently and accurately. Today, there is a large variety of underwater acoustics instruments. Sonar mapping systems can be roughly divided into three categories: single-beam echo-sounders, multi-beam echo-sounders and side-scan sonars [Blondel, 2009].

The tool of choice for high-resolution seabed mapping remains the side-scan sonar. Side-scan sonar is an instrument used to efficiently create an image of large areas of the sea floor (Figure1). This instrument covers a much larger portion of the seabed away from the surveying vessel, from a few tens of meters to 60 km or more. This coverage is attained by transmitting one beam on each side, broad in the vertical plane and narrow in the horizontal plane. Using different frequencies (from 6.5 kHz to 1 MHz), side-scan sonars achieve resolutions of 60 m down to 1 cm. The processing steps are less standardized, depending on the manufacturer, despite the consensus on the types of corrections desirable.

1.2 How side-scan sonars work

Side-scan uses a sonar device that emits conical or fan-shaped pulses down toward the sea floor across a wide angle perpendicular to the path of the sensor through the water, which may be towed from a surface vessel or submarine, or

mounted on the ship's hull. The intensity of the acoustic reflections from the sea floor of this fan-shaped beam is recorded in a series of cross-track slices. When stitched together along the direction of motion, these slices form an image of the sea bottom within the swath (coverage width) of the beam. The sound frequencies used in side-scan sonar usually range from 100 to 500 kHz; higher frequencies yield better resolution but smaller range.

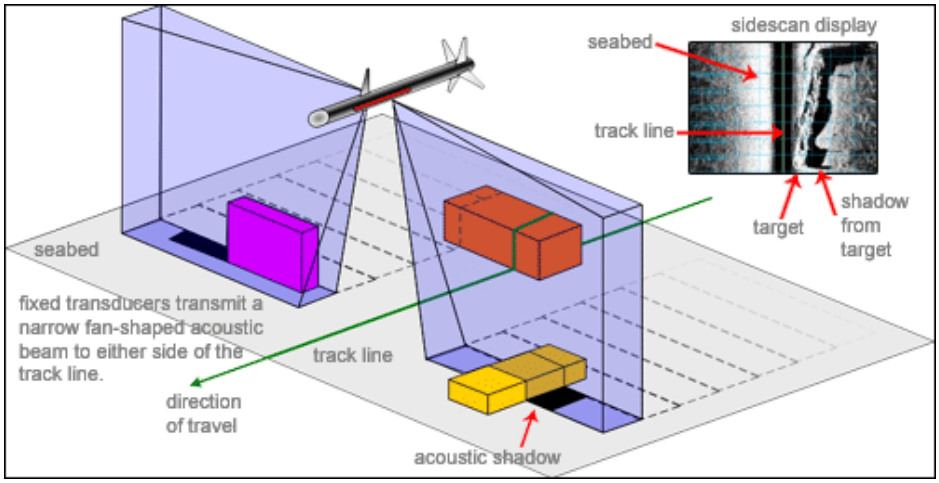

Figure 1: Side scan sonar principle

The reader should pay attention to the track line under the ship carrying the sonar and to the shadow generated by the beam, which impair image detection.

1.3 Applications

Side-scan sonar may be used to conduct surveys for maritime archaeology; in conjunction with sea floor samples it is able to provide an understanding of the differences in material and texture type of the seabed. Side-scan sonar imagery is also a commonly used tool to detect debris items and other obstructions on the sea floor that may be hazardous to shipping or to sea floor installations by the oil and gas industry. In addition, the status of pipelines and cables on the sea floor can be

investigated using side-scan sonar. Side-scan data are frequently acquired along with bathymetric soundings and sub-bottom profiler data, thus providing a glimpse of the shallow structure of the seabed. Side-scan sonar is also used for fisheries research, dredging operations and environmental studies. Military applications include reconnaissance, mine, H-Bomb and shipwreck detection.

2 Empirical mode decomposition

Empirical Mode Decomposition (EMD) is a time-frequency decomposition technique particularly suitable for non-stationary and non-linear signals [Huang et al., 1998]. EMD uses the intrinsic features of signals in the decomposition process; therefore, not only it is a fully data-driven method for signal processing, as well as, an adaptive, multi-scale and multi-resolution analysis method. Unlike spectrograms, wavelet analysis, or the Wigner-Ville distribution, HHT is a time-frequency analysis which does not require an *a priori* functional basis [Huang, 2005].

In the EMD process [Han \& Zhang, 2006], once the extrema of a time series signal x(t) are identified, all the local maxima and minima are interpolated by a cubic spline to form the so called upper and lower envelopes.

After signal decomposition by EMD, an intrinsic mode function (IMF) and a residue can be obtained. Then the continued decomposition goes on with the residue, and the new IMF and residue can be obtained. The operation does not stop until some conditions are met [S. Huang et al., 2012].

2.1 Advantages of EMD

EMD has some important advantages compared to Fourier transform [Zhidong and Yang, 2007] and Wavelet decomposition [Janusauskas et al., 2005].

The most important drawback of the Fourier Transform is that the signal is assumed to be stationary and linear, but in reality, most signals are neither linear, nor stationary. In the wavelet transform, it is possible to use different types of wavelets and the performance may change according to this selection.

Wavelet multi-scale analysis theory realize the scale adjustments via choosing different wavelet basis functions, and these basis functions are mutually independent. Furthermore, they have no connection with the concrete signal; therefore, it is very easy to lose some detailed information during processing [Huang et al., 1998].

On the other hand, EMD does not have basis functions and decomposes the signals based on their intrinsic properties. In the EMD method, the processed signal is decomposed into components called Intrinsic Mode Functions (IMFs) and a residue. The lower order IMFs capture fast oscillation modes (higher local frequency components) while higher order IMFs typically represent slow spatial oscillation modes (lower local frequency components). The residue reveals the lowest frequency general trend of the signal. IMFs can contain both high and low frequency details at different signal locations depending on signal characteristics. Every IMF must satisfy two conditions: first, the number of extrema (local maximum or local minimum) and the number of zero crossings are either equal or differ at most by one; and second, the average of the envelope defined by the local maxima and the envelope defined by the local minima is zero at all points [Huang et al., 1998].

The property of the above empirical mode decomposition is that it picks out the highest frequency oscillation that remains in the signal. Thus, locally, each IMF contains lower frequency oscillations than the one extracted just before. This property can be very useful to pick up frequency changes, since a change will appear even more clearly at the level of an IMF [Bougioukou et al., 2008].

Table 1 presents a concise comparison of Hilbert-Huang transform with Fourier and Wavelet transforms [Huang, 2005; Chung, 2014].

Table 1: Comparison of Fourier, Wavelet and Hilbert-Huang transforms

	Fourier	Wavelet	Hilbert - Huang
Basis	a priori	a priori	Adaptive
Frequency	Integral transform: Global	Integral transform: Regional	Differentiation: Local
Presentation	Energy-frequency	Energy-time-frequency	Energy-time-frequency
Nonlinear	no	no	yes
Non-stationary	no	yes	yes
Uncertainty	yes	yes	no
Harmonics	yes	yes	no

Source: chung EMD Tutorial 4.ppt

EMD has been applied widely in non-linearity and non-stationary signal processing such as speech, earthquake signals [Bougioukou et al., 2008], water wave signals [Ling et al., 2011; Manuel et al., 2008], etc.

2.2 BEMDecomposition

EMD has also been extended to two-dimension signal processing [Sancheza \& Trujillob, 2011; Xu et al., 2011].

A first approach is to transform a two-dimensional signal into a one-dimension vector, and then proceed with EMD. However, this way omits the spatial correlation of two-dimensional signals. Therefore, the bi-dimensional empirical mode decomposition (BEMD) has been proposed, and two-dimensional signals can be processed directly with BEMD. The details of EMD and BEMD decomposition can be found in the bibliography [S. Huang et al., 2012; Tasyapi Celebi and Erturk, 2010a; 2010b; 2012].

With BEMD, the applications of EMD have been extended to two-dimensional signals, such as image processing [Hariharan et al., 2006; Nunes and Delechelle, 2009; Xu et al., 2011; S. Huang et al., 2012].

3 Related work

The application of BEM Decomposition of side-scan sonar images is not new. From the recent bibliography we shall mention the works of S. Huang et al. (2012) and Tasyapi Celebi and Erturk (2010a).

In [Tasyapi Celebi and Erturk, 2010a] the authors propose a target detection algorithm for Side-scan sonar images based on Empirical Mode Decomposition (EMD) followed by morphological operations. According to the authors, the first IMF (IMF1) as well as the sum of the first two IMFs (IMF1+2) are first converted to binary images (using proper thresholds). Then, binary morphology is applied on each binary image. Finally the two resulting images are combined to obtain the final target detection result.

In [Tasyapi Celebi and Erturk (2010b)] the authors propose an EMD algorithm for image enhancement applied to poor quality underwater color images captured using optic cameras. The enhanced image is constructed by retaining the lower order IMFs that are multiplied by a set of weights to reconstruct the final image. Higher order IMFs that basically contain low-frequency underwater imaging impairments are discarded in this process.

It has been observed experimentally that the utilization of three IMFs provides the best performance. The weights used for the first three IMFs are fixed (0.7, 0.2 and 0.1) and have been yielded experimentally.

Ref. [Tasyapi Celebi and Erturk, 2012] is an improvement of [Tasyapi Celebi and Erturk, 2010b] where the weights of IMFs is carried out automatically using a genetic algorithm so as to optimize the sum of the entropy and average gradient of the reconstructed image. It was found that the proposed approach provides

superior results compared to conventional methods such as contrast stretching and histogram equalizing.

Huang et al. (2012) propose an image target detection algorithm for synthetic aperture radar (SAR) after analyzing the characteristics of EMD and SAR images. The proposed method performs EMD decomposition, feature extraction, election and fusion.

4 Methodology

In this paper, two methods for target detection with improved target detection accuracy in Side-scan sonar images are proposed.

In the first method, target detection is based on morphological operations; the second method is based on Empirical Mode Decomposition (EMD). Intrinsic Mode Functions (IMFs) are constructed by applying 2D EMD to side-scan sonar images.

4.1 Target detection based on morphological operations

The flow of the first method is as follows: First, the image is converted to black and white (binary image); Then, morphological operations are applied to clean the image, in particular, bridge, fill, clean and close [MATLAB, 1999; Marques, 2011; Amalorpavam, 2013]. Finally, edge detection filters are applied. Figure 2 provides a flowchart of the first method.

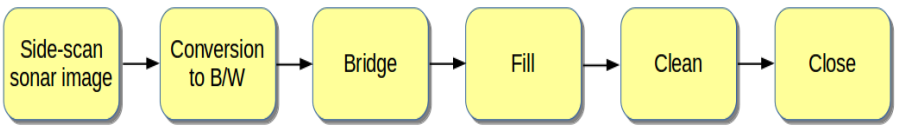

Figure 2: Target detection based on EMD Decomposition Flowchart

4.2 Target detection based on EMD Decomposition

The flow of the second method is as follows:

1. First, the image is decomposed into IMFs using BEMD decomposition;
2. The first four IMFs are calculated;
3. The weighted sum of IMFs 1+2, 1+3, 1+2+3, 2+3+4 is calculated;
4. These combined IMFs are converted to black and white images using proper thresholds;
5. Morphology operations are applied (close);
6. Edge detection filters are applied.

The weights used for the IMF combinations are fixed and have been calculated experimentally. In particular, they are as follows:

- IMF 1+2 = 0.7*IMF1 + 0.3*IMF2;
- IMF 1+3 = 0.6*IMF1 + 0.4*IMF3;
- IMF 1+2+3 = 0.5*IMF1 + 0.4*IMF2 + 0.1*IMF3;
- IMF 2+3 = 0.5*IMF2 + 0.5*IMF3;
- IMF 2+3+4 = 0.5*IMF2 + 0.3*IMF3 + 0.2*IMF4.

Edge detection is important in order to prepare the image for further processing, such as pattern recognition [Huaxin et al., 2011].

Figure 3 provides a flowchart of the second method.

By principle, the first IMF contains the highest frequencies whereas the next IMFs hold decreasingly lower frequencies, and the last IMF contains a constant component [Huang, CHAPTER 1]. As a consequence, if the original image contains high-frequency noise (as is the usual case), then this noise will be present in the first IMF. By including the first IMF in the final image, we also introduce the high-frequency noise. Hence, in case of noisy images, the 1st IMF could be avoided or used with a low weight factor!

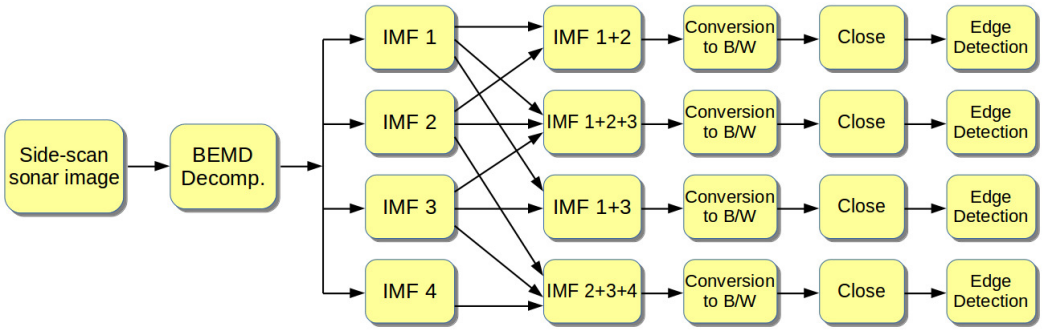

Figure 3: Target detection based on EMD Decomposition Flowchart

5 Results

5.1 Test images

Results for two different test images are presented:

Table 2: Test images

Image	Resolution	Size	Remarks/Challenges
Boat (boat1gray.jpeg)	72x72 ppi Grayscale	289x156 pixels 45084 pixels, 39,6 kB	Strong shadow
Plane (plane1gr.jpeg)	72x72 ppi Grayscale	282x177 pixels 49914 pixels, 28,6 kB	Strong shadow Varying illumination

Figure 4 presents test image1 ``boat''. A special feature of this image is the strong shadow which produces erroneous image perception and edge detection.

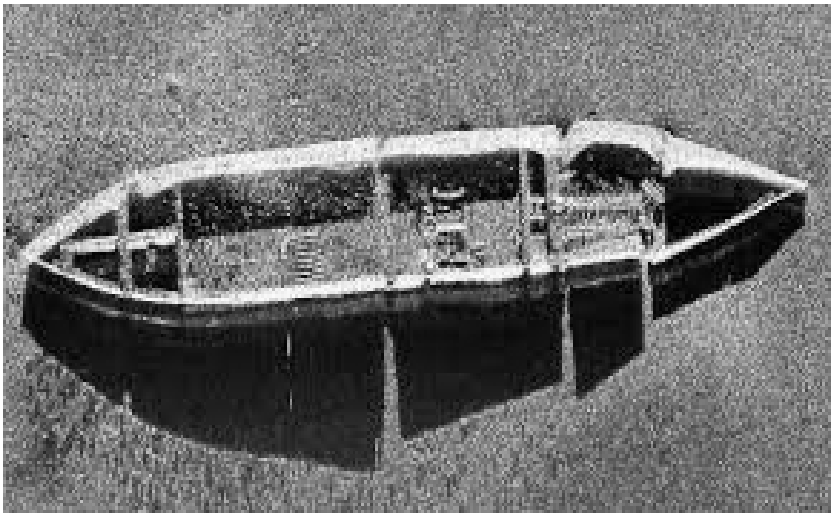

Figure 4: First test image: "boat"

Figure 5 presents the second test image "plane". Additional special features which prevent correct image perception and target recognition (beyond the strong shadow), are: (a) the sub-illuminated spindle; (b) the over-illuminated front part of the wings; (c) the different illumination of the background (possibly due to the track line) and (d) the artifacts at the top of the image.

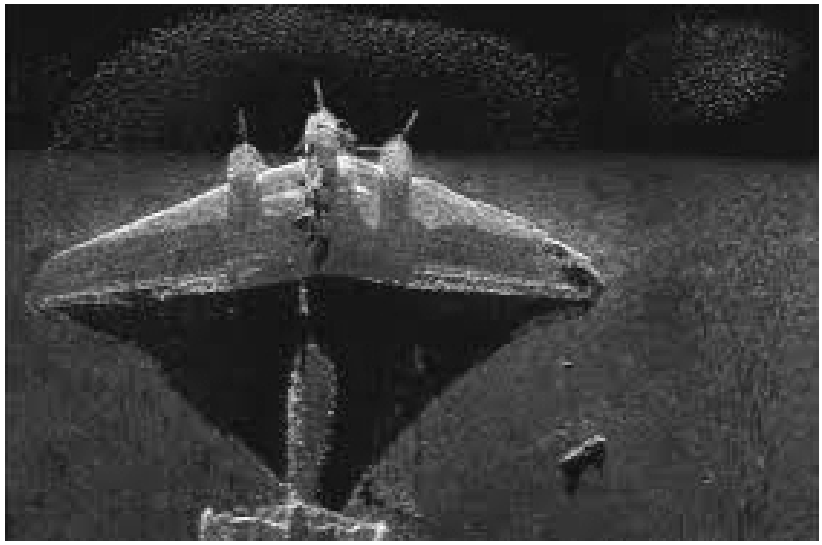

Figure 5 : Second test image: "plane"

5.2 Method 1

Figure 6 presents the result of the first method on test image boat:

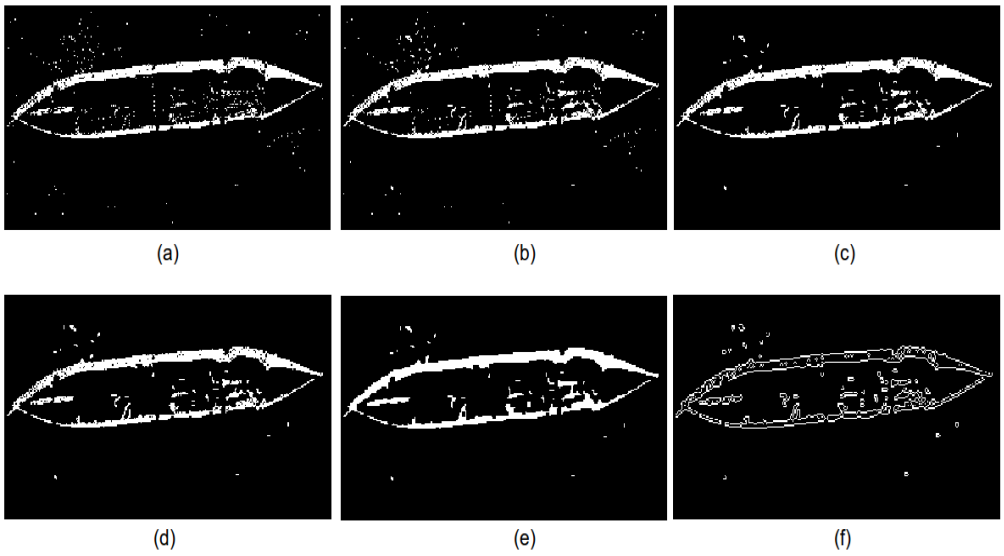

Figure 6: Boat: result of the 1st method. (a) Binary image; (b) After bridge; (c) After fill; (d) After clean; (e) After close; (f) After Sobel filter

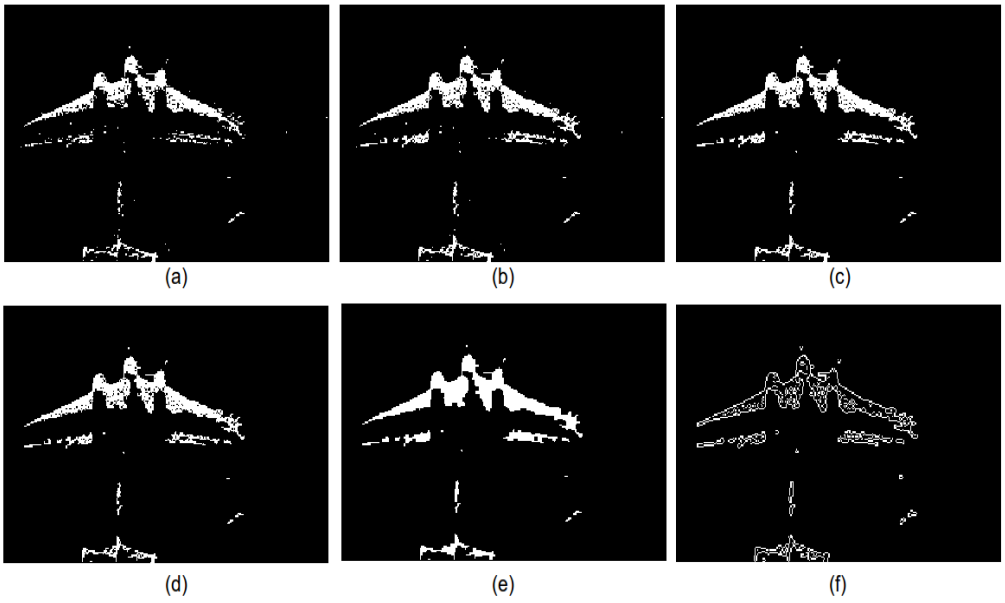

Figure 7: Plane: result of the 1st method. (a) Binary image; (b) After bridge; (c) After fill; (d) After clean; (e) After close; (f) After Sobel filter on image (c)

As we can see, method 1 manages to dispose of the shadow, due to proper thresholding. The next steps emphasize the outline of the object. Result (e) is remarkably better than that of a typical edge detection filter (f). Figure 7 presents the results of the first method on test image "plane".

Figure 8 presents the effect of edge detection filters on result of the 1st method on test image **plane.**

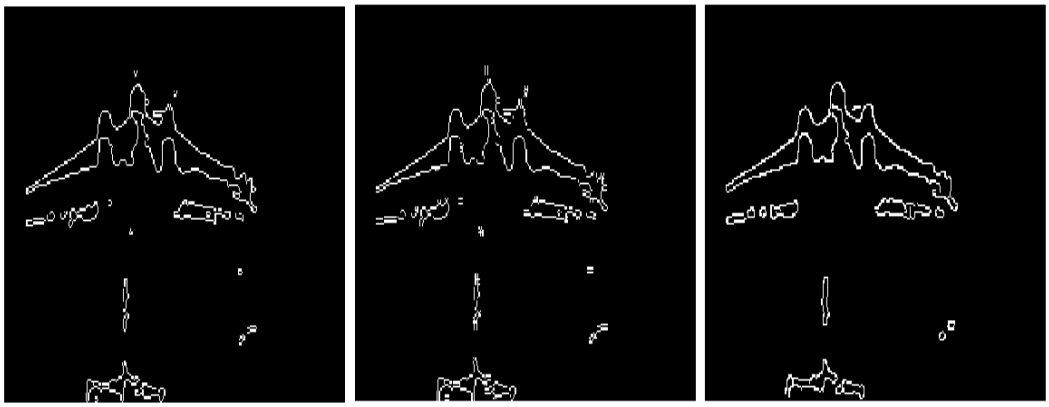

Figure 8: Edge detection of **plane image** (e): (a) Sobel filter; (b) Prewitt filter; (c) Canny filter

As we can see, due to the particular features of test image ``plane", the results are somewhat inferior than those of test image ``boat": the spindle is not evident and the upper part of the wings is very bright. Edge detection does not provide better results. Target recognition might fail.

5.3 Method 2

5.3.1 Boat: results of the 2nd method

Next, results from the second method will be presented, starting with test image boat.

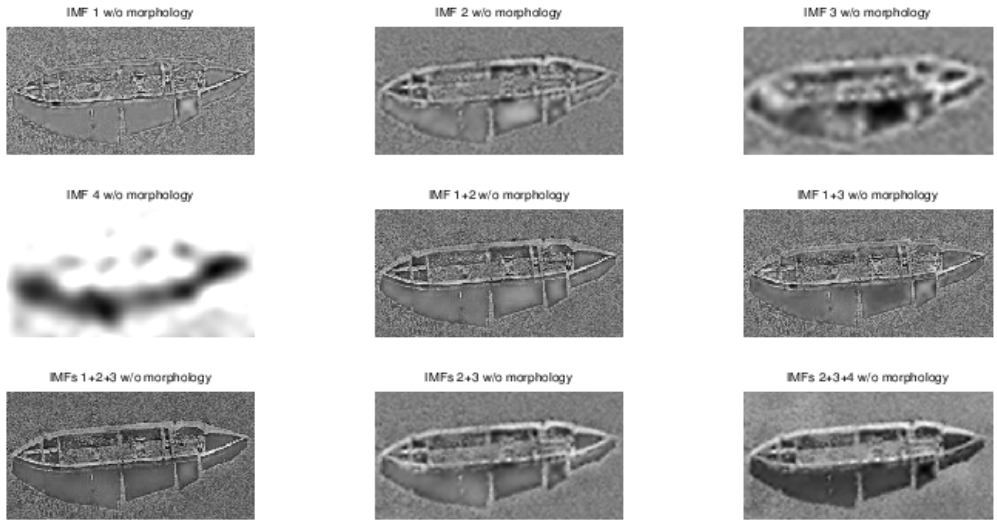

Figure 9: Boat: results of the 2nd method

From Figure 9 we observe that BEMD was unable to remove the shadow; this is the reason for using thresholding and morphology.

In Figure 10 we can see that the next steps of method 2 managed to get rid of the shadow; however, results seem worse than those of method 1.

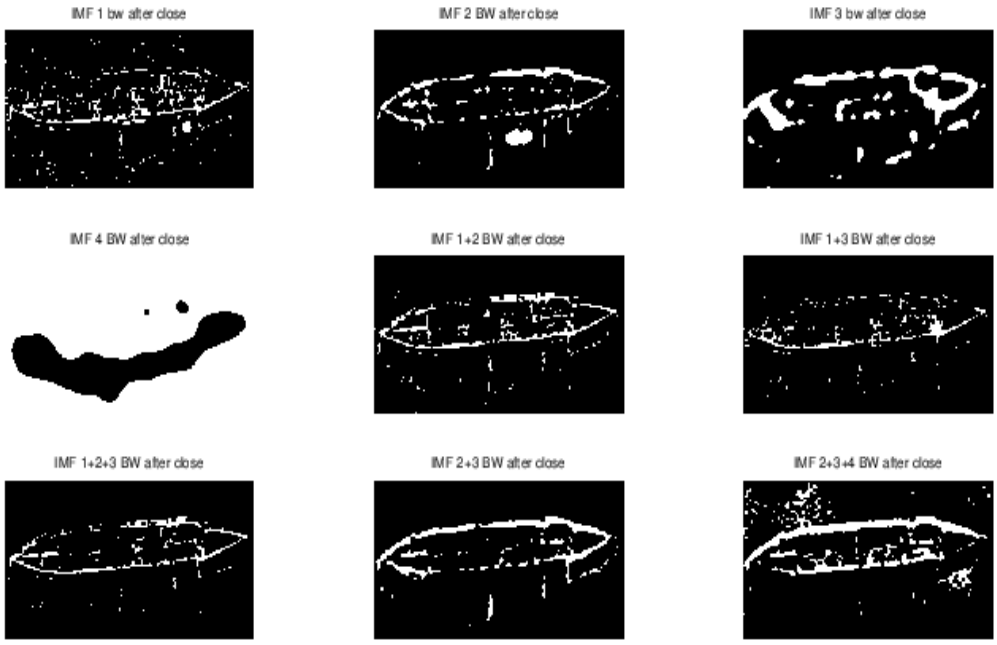

Figure 10: Boat: results of the 2nd method: binary images

5.3.2 Plane: results of the 2nd method

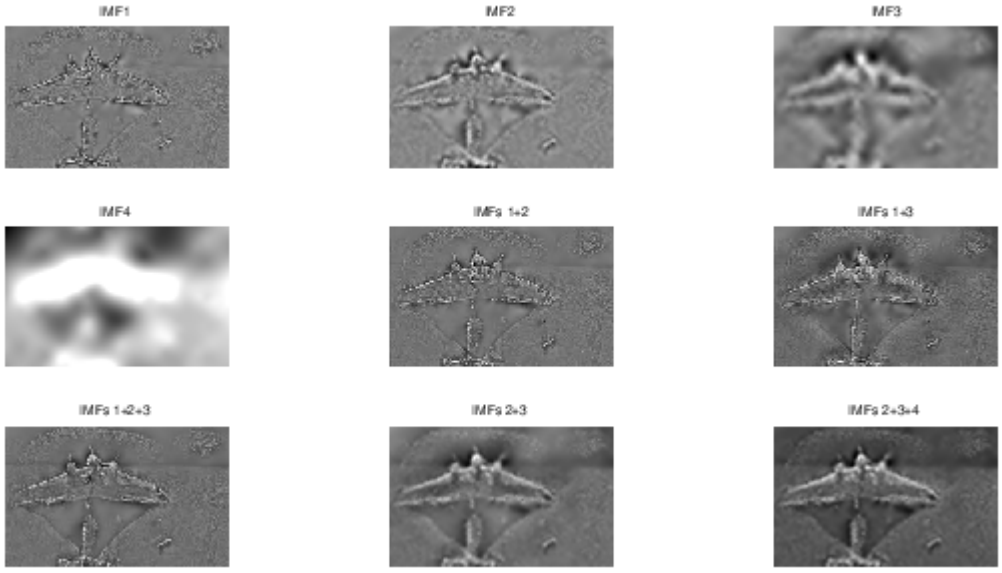

Figure 11: Plane: results of the 2nd method (Grayscale)

In Figure 11 we observe that some IMF combinations (e.g., 2+3 and 2+3+4) manage to extract the shape of the plane. The thresholding steps of method 2 (Figure 12), especially IMFs 2+3+4, provide a satisfactory result.

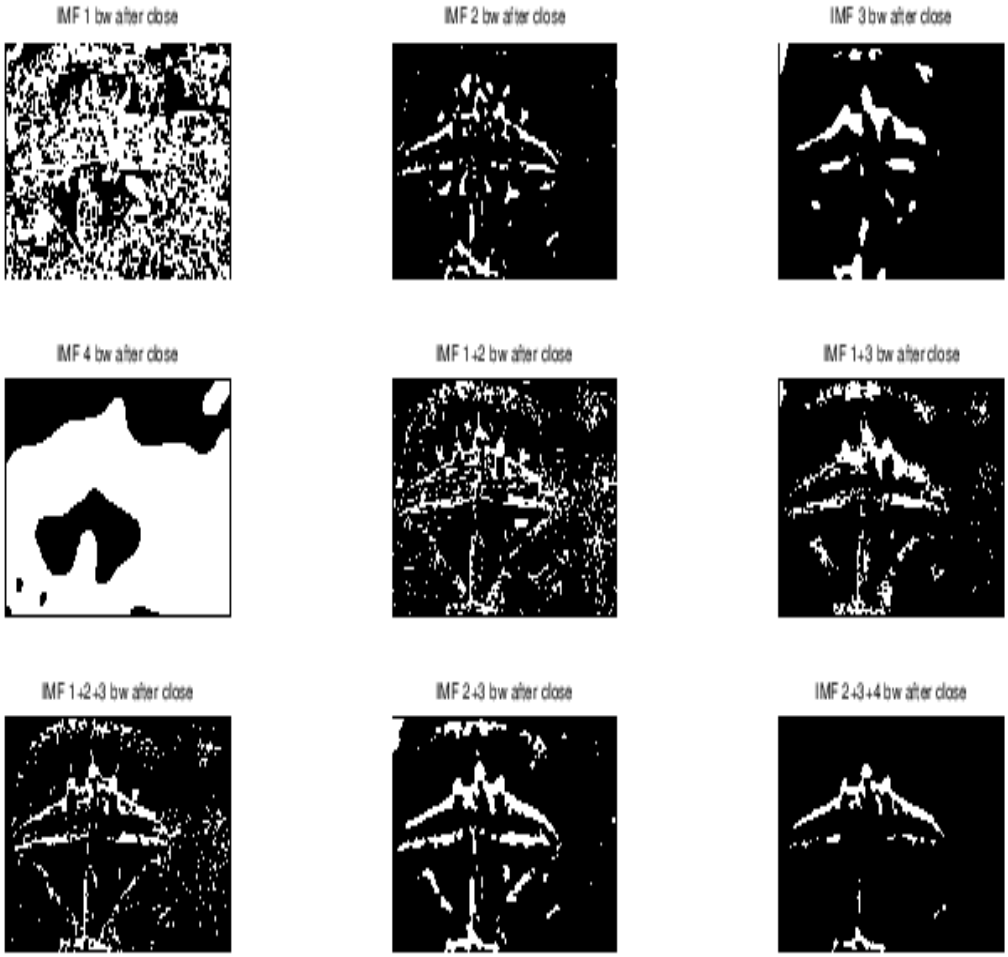

Figure 12: Plane: results of the 2nd method (binary)

Edge detection filters applied on the results of the previous steps also provide satisfactory results (Figure 13).

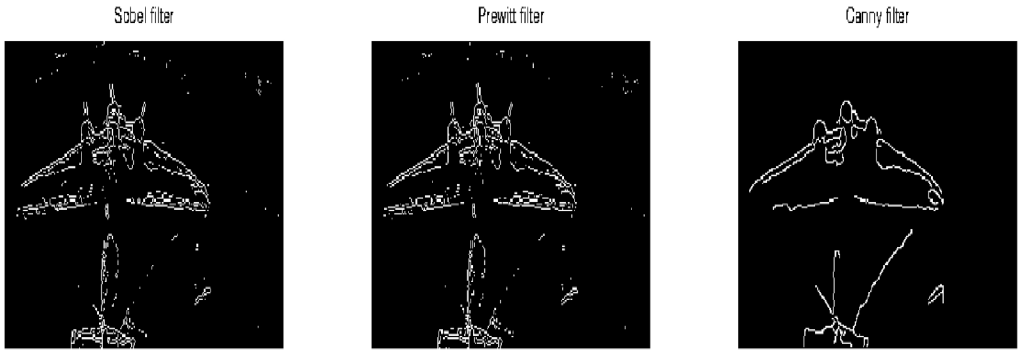

Figure 13: Plane: results of the 2nd method (edge detection)

5.4 Findings

From the examples demonstrated we conclude that:

1. According to the input image, one or the other method may provide better results.
2. Threshold selection for grayscale to binary image conversion is critical. Small changes in threshold values may lead target detection in failure.
3. The thresholds for converting the grayscale images to binary are automatically calculated using the method proposed by Otsu [Otsu, 1979; Marques, 2011]. However, the Otsu thresholds worked only for the plane test image; the thresholds had to be incremented significantly for the boat test image. Slight increments to the Otsu thresholds improved results also for the *plane* test image.
4. Target detection is greatly facilitated by a set of images, both grayscale and binary, instead of using just a single image.
5. Morphology on IMF combinations filters out the shadow and presents the outline of the object even in cases where classical edge detection filters fail (for example: boat and IMFs 1+3).
6. If the image has a lot of details and noise, we may have to reject the first IMF

in favour of clearness.

7. Usually IMF combinations 1+2 and 1+2+3 after morphology provide better edge detection and present correctly the outline of the object. This observation has been verified with many test images.
8. Thus, for best target detection results, we propose a combination of two different approaches running in parallel.

6 Conclusions

In this paper, two methods for target detection with improved target detection accuracy in side-scan sonar images have been proposed. The first method is based on morphological operations and edge detection whereas the second method is based on BEMD decomposition followed by morphological operations and edge detection. Three edge detection filters have been used: Sobel, Canny and Prewitt.

The thresholds for converting the grayscale images to binary are automatically calculated using Otsu's method. However, it was found experimentally that the calculated threshold values should be increased (more or less) for best results.

Experimental results indicate that the proposed methods are very effective, but their efficiency depends on the features of the input image.

Depending on the image, one or the other method may produce the best results.

Processing time of the first method is considerably shorter than that of the second one, because EMD decomposition takes time.

We support that the two methods presented here should be used in parallel for optimal target detection.

References

[1] P. Blondel, *The Handbook of Sidescan Sonar*, Springer 2009.

[2] N.E. Huang, Z. Shen, S.R. Long, M.C. Wu, H. H. Shih, Q. Zheng, N-C. Yen, C. C. Tung and H. H. Liu, The empirical mode decomposition and the Hilbert Spectrum for nonlinear and non-stationary time series analysis, *Proc. R. Soc. London*, A., **454**, (1998), 903-995.

[3] D. Han and S.-N. Zhang, Comparison between windowed FFT and Hilbert–Huang transform for analysing Time series with Poissonian fluctuations: A case study, arXiv:astro-ph/0609012V1, 1 September, 2006.

[4] N.E. Huang, *Introduction to the Hilbert-Huang Transform and its Related Mathematical Problems*, in N. E. Huang and S. S. P. Shen (Eds), Hilbert-Huang Transform and its Applications, World Scientific, Sept. 2005.

[5] Z. Zhidong and W. Yang, A new method for processing end effect in empirical mode decomposition, *International Conference on Communications, Circuits and Systems*, Kokura, Japan, (2007), 841-845.

[6] A. Janusauskas, R. Jurkonis, A. Lukosevicius, S. Kurapkiene and A. Paunksnis, The empirical mode decomposition and the discrete wavelet transform for detection of human cataract in ultrasound signals, Informatica, Lith. Acad. Sci., **16**(4), (2005), 541-556.

[7] A.P. Bougioukou, A. P. Leros and V. Papakonstantinou, Modeling of non-stationary ground motion using the mean reverting stochastic process', *Applied Mathematical Modelling*, **32**, (2008), 1912-1932.

[8] E. Chung, Tutorial on the Empirical Mode Decomposition Method (EMD), 2014. www. math.cuhk.edu.hk/ course/math3290/Tutorial\%204.ppt.

[9] H. Ling, L. Margaret, C. M. Namunu and B. A. Nicholas, Study of empirical mode decomposition and spectral analysis for stress and emotion classification in natural speech, *Biomedical Signal Processing and Control*, **6**(2), (2011), 139-146.

[10] B.V. Manuel, W. Binwei and E. B. Kenneth, ECG signal denoising and

baseline wander correction based on the empirical mode decomposition, *Computers in Biology and Medicine*, **38**(1), (2008), 1-13.

[11] J.L. Sanchez and J. J. Trujillo, Improving the empirical mode decomposition method, *Applicable Analysis*, **90**(3-4), (2011), 689-713.

[12] G.L. Xu, X. T. Wang and X. G. Xu, Improved bi-dimensional empirical mode decomposition based on 2d-assisted signals: analysis and application, IET *Image Processing*, **5**(3), (2011), 205-221.

[13] S. Huang, B. Wang, Y. Li and B. Ge, SAR Target Detection Method Based On Empirical Mode Decomposition, *Advanced Engineering Forum*, **6-7**, (2012), 496-500.

[14] A.T. Celebi and S. Erturk, ``Target Detection in Sonar Images Using Empirical Mode Decomposition and Morphology". Undersea Defence Technology (UDT) Europe 2010, accepted for presentation, 2010.

[15] A. T. Celebi and S. Erturk, ``Empirical mode decomposition based visual enhancement of underwater images, 2nd *International Conference on Image Processing Theory Tools and Applications* (IPTA 2010), 221-224.

[16] A.T. Celebi and S. Erturk, Visual enhancement of underwater images using Empirical Mode Decomposition, *Expert Systems with Applications*, **39**(1), (January, 2012), 800-805.

[17] H. Hariharan, A. Gribok, M. A. Abidi and A. Koschan, Image fusion and enhancement via empirical mode decomposition', *Journal of Pattern Recognition Research*, **1**(1), (2006), 16-32.

[18] J.-C. Nunes and E. Delechelle, Empirical Mode Decomposition: Applications on signal and image processing, *Advances in Adaptive Data Analysis*, **1**(1), (2009), 125-175.

[19] MATLAB Image Processing Toolbox User's Guide, Ver. 2, January 1999.

[20] A. Tan, Hilbert-Huang Transform, 23 Apr. 2008, MATLAB File Exchange. Accessed: 24 Jan. 2015.

[21] O. Marques, Practical Image and Video Processing using MATLAB,

Wiley/IEEE, 2011.

[22] G. Amalorpavam, T. Harish Naik, Jyoti Kumari and M. Suresha, Analysis of Digital Images Using Morphological Operations, *International Journal of Computer Science and Information Technology* (IJCSIT), 5(1), (February, 2013), 145- 159. DOI : 10.5121/ ijcsit.2013.5112.

[23] Z. Huaxin, Z. Huigang, B. Xiao and Z. Huijie, Query Expansion for VHR Image Detection, *Proceedings of* IGARSS 2011, 205-209.

[24] N. Otsu, A threshold selection method from gray-level histograms, IEEE *Transactions on Systems, Man, and Cybernetics*, **9**(1), (1979), 62-66.